Journal of Marine Systems 230 (2022) 103733

Contents lists available at ScienceDirect

Journal of Marine Systems

journal homepage: www.elsevier.com/locate/jmarsys

Mid-summer vertical behavior of a high-latitude oceanic zooplankton community

Kanchana Bandara [a,*], Sünnje L. Basedow [a], Geir Pedersen [b], Vigdis Tverberg [c]

[a] Department of Arctic and Marine Biology, Faculty of Fisheries, Biosciences and Economics, UiT – The Arctic University of Norway, 9037 Tromsø, Norway
[b] Department of Ecosystem Acoustics, Institute of Marine Research, PO Box 1870, Nordnes, 5817 Bergen, Norway
[c] Faculty of Biosciences and Aquaculture, Nord University, Bodø 8049, Norway

ARTICLE INFO

Keywords:
Diel vertical migration
Zooplankton schooling
Zooplankton swarms
Calanus
Plankton acoustics
Autonomous surface vehicles
Sailbuoy
Ocean gliders

ABSTRACT

Vertical behavior, such as diel vertical migration (DVM) and swarming are widespread among zooplankton. At higher latitudes, synchronized DVM is mostly absent during summer and predominantly herbivorous copepods tend to form large near-surface swarms. This behavior is risky because it can make them vulnerable to visual predators. Here, we used ca. 12 days of mid-summer (28 June to 10 July 2018) high-frequency acoustic data collected on board of an autonomous surface vehicle (Sailbuoy) to study the vertical behavioral patterns of a zooplankton community in the Norwegian Sea (69°–71° N). Comparing acoustic data with zooplankton net samples, we could distinguish the sound scatters into (1). lipid-rich older developmental stages of *Calanus* spp., (2). younger developmental stages of *Calanus* spp., smaller copepods and krill and (3). unknown group of strong sound scatters that may have been younger stages of planktivorous fish. We observed shorter-range classic DVM during much of the study period, where in two days, the migration appeared to be pronounced (> 50 m in amplitude), largely synchronous and occurred in the presence of sound scatterer group 3. The observed zooplankton community was concentrated in the upper 20 m in cloudy and calm days but retreated to greater depths at increased near-surface turbulence. This turbulence-driven vertical retreat appeared to be synchronized across the zooplankton community, potentially indicating a schooling behavior.

1. Introduction

Zooplankton represent the heterotrophic component of the plankton community, which include a diversity of mostly microscopic aquatic organisms that cannot usually swim against a water current (in Greek, *planktos* = drifter). Despite their restricted lateral movements, most zooplankton can actively adjust their vertical position in the water column through a variety of swimming patterns (Saiz, 2009). These 'vertical behaviors' are among the most studied patterns of animal behavior. Two widespread types of zooplankton vertical behaviors include Diel vertical migration (DVM) and swarming (Price et al., 1988).

Diel vertical migration (DVM) reflects the tendency of zooplankton to occupy different parts of the water column (i.e., vertical habitats) during different times of the day (Bayly, 1986; Brierley, 2014; Bandara et al., 2021). The most common (classic) type of DVM typically signifies the occupation of near-surface waters by zooplankton during nighttime and deeper waters during the day. Irradiance (in the visible and ultraviolet spectral ranges) is considered as the main proximate cue for zooplankton DVM (Cohen and Forward, 2009; Williamson et al., 2011). This irradiance-induced behavior allows predominantly herbivorous zooplankton to feed in the productive near-surface waters during nighttime when light-dependent visual predation risk is minimal and to take refuge in deeper darker waters where the detection efficiency of visual predators is hampered during daytime (Lampert, 1989). On the other hand, swarming is the formation of monospecific zooplankton aggregates that are diverse in spatial and temporal scales (Omori and Hamner, 1982; Folt and Burns, 1999; Seuront et al., 2004). Zooplankton densities within a swarm can be several orders of magnitude greater compared to the background levels, within which individuals may exhibit synchronized orientation (schooling) (Omori and Hamner, 1982). The proximate cues of swarming vary considerably between zooplankton taxa, which could be a true behavior controlled by

Abbreviations: DVM, Diel vertical migration.

* Corresponding author.
E-mail addresses: info@kanchanabandara.com (K. Bandara), sunnje.basedow@uit.no (S.L. Basedow), geir.pedersen@hi.no (G. Pedersen), vigdis.tverberg@nord.no (V. Tverberg).

https://doi.org/10.1016/j.jmarsys.2022.103733
Received 30 November 2021; Received in revised form 1 March 2022; Accepted 15 March 2022
Available online 18 March 2022

environmental variability (changes of irradiance, temperature, dissolved gases and salts and perception of food and predators) or a passive aggregation driven by physical retentive processes (Ambler, 2002). Although the adaptive significance of swarming is not well understood, it may enhance mate selection, geographical retention or dispersal and may also act as an antipredator mechanism (Ohman, 1988; Folt and Burns, 1999; Ambler, 2002).

Vertical behavior of high-latitude zooplankton is of particular interest because of its seasonal variability. The intensity of DVM fluctuates seasonally, from a pronounced synchronized pattern during spring and autumn (when the diel variability of light is most pronounced) to a diminished asynchronized pattern during the rest of the year (Cottier et al., 2006; Wallace et al., 2010; Darnis et al., 2017). The lack of DVM during the high-latitude winter (polar night) is somewhat obvious; first, due to the diminished light-dependent (visual) predation risk and second, because most herbivorous zooplankton vacate the upper pelagial and overwinter (in a state of hibernation termed 'diapause') typically at greater depths (Baumgartner and Tarrant, 2017; Bandara et al., 2021). A peculiar observation made during high-latitude summer (the period of midnight sun) is that some herbivorous zooplankton – particularly copepods of the genus *Calanus* - do not perform notable DVM (Blachowiak-Samolyk et al., 2006; Basedow et al., 2010) and occupy the near-surface in dense swarms, which are sometimes observable from space (Basedow et al., 2019). The adaptive significance of this near-surface swarming is questionable because it makes the copepods easier targets of visual predators, whose detection efficiency is maximal at the upper pelagial during summer (period of midnight sun).

One hypothesis about the lack of synchronized DVM during the period of midnight sun relates to the reduced diel variations of irradiance perceived by zooplankton (Cottier et al., 2006). However, considerable changes in the light regime occur throughout the diel cycle in most high-latitude settings (Campbell and Aarup, 1989). On top of this, shorter-term changes of cloud cover may also momentarily attenuate the subsurface light regime. These shorter-term irradiance variations should offer a sufficient proximate cue for zooplankton to perform DVM (see Omand et al., 2021) because some herbivorous copepods and krill are sensitive to finer variations of light (Cohen and Forward, 2002; Båtnes et al., 2015). In fact, recent observations suggest that some high-latitude zooplankton communities follow preferred light intensities (irradiance isolumes) year-round, showing that there are perceivable levels of irradiance across the seasons (Hobbs et al., 2021). Nonetheless, the typical absence of synchronized DVM even under the presence of perceivable diel variations of irradiance points to an alternative hypothesis that there is no adaptive benefit of performing DVM during the period of midnight sun (Basedow et al., 2008). Vertical migration can be energetically demanding, particularly when it involves crossing sharp density gradients (Lampert, 1989). DVM also shrinks the daily feeding window and may hamper growth, development and reproductive rates (Stich and Lampert, 1984; Hays et al., 2001; Bandara et al., 2018). Empirical evidence from both marine and freshwater systems suggests that when visual predators are absent, zooplankton may abandon these costly diel vertical excursions and occupy the food-rich upper pelagial throughout the day (e.g. Bollens and Frost, 1989b; Dini and Carpenter, 1992). DVM may commence or occur with greater intensity when predators are present in the habitat and perceived by zooplankton via mechanical or chemical signals (Bollens and Frost, 1989a; Loose and Dawidowicz, 1994).

In this study, we focus on understanding mid-summer vertical behavioral patterns of a high-latitude oceanic zooplankton community (predominantly, *Calanus* spp.) in the Norwegian Sea (69–71° N). We base our study on ca. 12 days of high-frequency acoustic data collected between late June and mid-July on board an autonomous surface vehicle. Using this data, we attempt to identify different patterns of vertical behavior exhibited in the zooplankton community, such as DVM and swarming. We use zooplankton net samples to groundtruth the acoustic data towards resolving the identities of responsible actors of above vertical behaviors. Using physical (irradiance, near-surface turbulence) and biological (presence of potential predators) environmental variables, our objective is to characterize the potential proximate drivers and adaptive significance of the observed vertical behavioral patterns.

2. Materials and methods

2.1. Study area

This study was conducted in open waters off the northern Norwegian shelf (Fig. 1). The depth of the study area exceeds 2000 m, and to the southeast, this deep seabed is connected to a narrow continental shelf via a steep slope (Fig. 1). While the northeasterly-flowing Norwegian Coastal Current (NCC) advects low-saline water along the shelf, the main branch of relatively warm and high-saline Atlantic water, termed the Norwegian Atlantic Current (NwAC) flows northwards along the shelf slope (Skarðhamar and Svendsen, 2005). Routine cross-shelf exchange and mixing of these water masses are influenced by a system of cross-shelf trenches and banks (Sundby, 1984; Moseidjord et al., 1999). Thermohaline stratification of these water masses in combination with the seasonal availability of light and nutrients trigger dense phytoplankton blooms in the region (Rey, 2004; Sakshaug et al., 2009). A myriad of consumers, i.e., planktonic grazers, planktivorous and piscivorous fish, marine mammals and seabirds transfer the energy from primary producers across the pelagic food web (Gjøsæter, 1995; Vadstein, 2009).

2.2. In-situ observation of the zooplankton community

Central to this study was a silent autonomous surface vehicle – the Sailbuoy (Offshore sensing A/S: www.sailbuoy.no) that was deployed along the northern Norwegian shelf between spring and autumn of

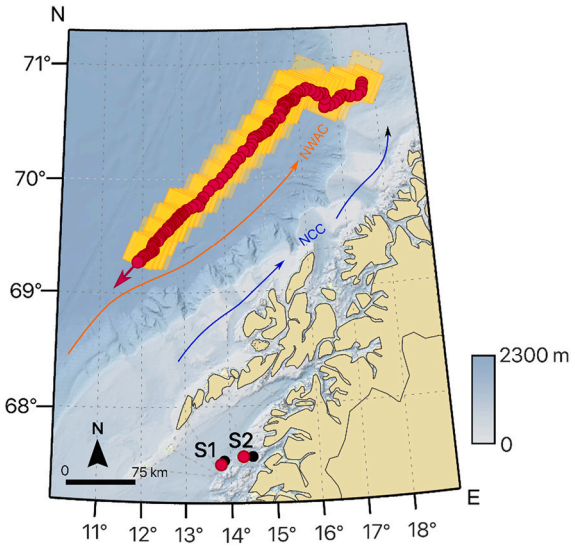

Fig. 1. Map of the study area. The autonomous platform equipped with acoustic sensors (Sailbuoy) followed a southwesterly course as indicated by the red circles (waypoints recorded in the autopilot system) and the red arrow. The 0.25° × 0.25° grids from which time-specific total cloud cover data were extracted from ERA-Interim reanalysis archives are marked with yellow squares along the Sailbuoy track. S1 and S2 (black dots) are the two sampling stations from which zooplankton net samples and environmental variables were collected for groundtruthing of acoustic data. The red dots near the sampling stations are positions of the Sailbuoy during sampling. NwAC = Norwegian Atlantic Current, NCC = Norwegian Coastal Current. Bathymetric data from the 'mareano' project (http://mareano.no/kart/). (For interpretation of the references to color in this figure legend, the reader is referred to the web version of this article.)

2018. The Sailbuoy was equipped with a Simrad™ compact wideband transceiver WBT Mini® (Kongsberg Maritime A/S), which is a power-efficient broadband echosounder. The echosounder was connected to an ES333-7CD transducer with an operational frequency range of 283–383 kHz. The echosounder transducer was mounted on a bulb on the Sailbuoy's keel ca. 0.5 m below the waterline. It transmitted pulses with a theoretical beam opening angle of 7° (−3 dB) at 1 ms duration with a repetition rate of 2 s. The Sailbuoy's properties together with the higher operating frequency range of the transducer make it well-suited for monitoring larger aggregations of zooplankton down to 50–100 m depth (Pedersen et al., 2019).

For this study, we used mid-summer echosounder data from 29 June 00:00 h to 10 July 10:00 h Central European Summer Time (GMT + 2) collected during the 2018 Sailbuoy deployment. During this period, the Sailbuoy was on a near-linear southwesterly course (Fig. 1). Although the Sailbuoy moved on the continental shelf at the initial part of its course, it travelled across the deeper waters during most of its voyage (Fig. 1). However, the sea bottom always remained deeper than the maximum vertical coverage of the echosounder (≈ 150 m) during the voyage. The echosounder data were not sampled continuously, as the transducer was active ('on' state) only for six minutes each hour (equivalent duty cycle of ca. 10%) to conserve power and storage space. Since all these echosounder data chunks were recorded at the onset of each hour (i.e., 0th minute to the 6th minute), this provided consistent hourly snapshots of the zooplankton community.

2.3. Sampling of the zooplankton community

To resolve the identity of the sound scatterers in the echosounder data (groundtruthing), we sampled the zooplankton community at two different stations when the Sailbuoy was in close proximity (S1 and S2: Fig. 1). The two stations were sampled at mid-day on 26 April and 28 May 2018, respectively. Sampling was done on board R/V 'Tanteyen' of Nord University using a MultiNet midi (Hydrobios, Germany) with a mesh width of 180 μm and a mouth opening of 0.25 m^2. The net was towed vertically at a constant upward velocity of ca. 0.5 m s^{-1} across two discreet depth layers, 50–20 m and 20–0 m. Since no conspicuous individuals, such as larger jellyfish and ctenophores were captured, entire samples were labelled and preserved in borax-buffered 4% formaldehyde-in-seawater solution until further processing in the laboratory.

In the laboratory, samples were rinsed and split into fractions using a box splitter (1/4 split for 26 April samples, 1/32 split for 28 May samples). From these sub-samples, aliquots of 2.5 ml were scanned under a Leica™ stereo microscope (Leica Microsystems inc.) for identification, enumeration and measurement of collected zooplankton. As *Calanus* spp. were the most common in all samples, the identification was carried out until 300 *Calanus* spp. individuals (at any developmental stage) and 150 individuals of other taxa were encountered. For rare taxa (< 5 individuals per sample), the entire sample was scanned. Wherever possible, individuals were identified to genus or species levels. *Calanus* spp. were classified according to their developmental stages (i.e., naupllii, copeodites I—V, adult male and female). All individuals were measured for their body length (i.e., prosome length for copepods, total length for others) and maximum body width. Diameter was measured for those with globular body shapes, such as fish eggs and gastropods. All measurements were made at 0.1 mm resolution.

2.4. Environmental variables

The water column of the two sampling stations (S1 and S2) was profiled for temperature, salinity and Chlorophyll-*a* biomass (fluorescence) using a SAIV SD204 CTD device with an affixed fluorometer (SAIV A/S). Although subsurface environmental data were not collected during the Sailbuoy's voyage, near-surface temperature and salinity were measured using a NBOSI hull-mounted CT sensor (Neil Brown Ocean Sensors inc.). We supplemented these environmental data with space- and time-specific estimates of total cloud cover along the Sailbuoy track (0.25° spatial and 3 h temporal resolution) extracted from the European Centre for Medium-Range Weather Forecasts (ECMWF) ERA-Interim reanalysis archives (Berrisford et al., 2011). The 3 h temporal resolution of total cloud cover estimates was adjusted to an hourly resolution by spanning the gaps using linear interpolation. We used the global clear-sky horizontal irradiance model of Robledo and Soler (2000) to estimate space- and time-specific estimates of photosynthetically active radiation (PAR) along the Sailbouy track at hourly resolution. These clear-sky PAR estimates $[(PAR_{cs})_{t,z=0}]$ were attenuated with the total cloud cover estimates (C) to obtain an approximate estimate of incident irradiance at the sea surface $[(PAR)_{t,z=0}]$ as,

$$(PAR)_{t,z=0} = 0.72 \bullet C_t \bullet (\mathrm{PAR_{cs}})_{t,z=0} \quad (1)$$

Here, t and z are time and depth, respectively. The attenuation coefficient (0.72) was selected in a way that the estimated PAR matches those extracted from ERA-Interim reanalysis archives. However, we did not use the reanalysis PAR data in our study, because its temporal resolution was coarse (6 h).

The lack of subsurface environmental data along the Sailbuoy track did not warrant an accurate estimation of subsurface sound speed, which varies with thermohaline properties of seawater and the hydrostatic pressure (Wilson, 1960) and may influence the qualitative and quantitative characterization of sound scatterers (see below). As a rough measure to address this, we used in-situ contemporary temperature and salinity measurements from a Seaglider (Kongsberg Maritime A/S) operating ca. 240–420 km away from the Sailbuoy to create a hypothetical subsurface sound speed profile along the Sailbuoy track (Appendix A). Although the accuracy of these predictive estimates remains unknown (due to lack of in-situ data for cross-validation), we believe that it provided a better acoustic characterization of sound scatterers than that based on a constant sound speed calculated from near-surface thermohaline estimations.

2.5. Processing of acoustic data

2.5.1. Pre-processing

Acoustic data were processed using ESP3 (version 1.9.9) – an open-source software package for visualization and processing of acoustic data developed by the deep-water fisheries acoustics team at the National Institute of Water and Atmospheric Research (NIWA), New Zealand (Ladroit et al., 2020). Acoustic data were imported into ESP3 as .RAW files. Estimated subsurface temperature and salinity data (.CNV files based on Seaglider data: see Appendix A) were imported separately, and depth- and time-specific sound speed profiles were created in ESP3 following Francois and Garrison (1982). The imported acoustic data did not have any geographical metadata because the echosounder does not accept navigational inputs (e.g., from the Sailbuoy's autopilot system: Pedersen et al., 2019). We therefore imported the time-specific longitude and latitude data (.CSV files) from the Sailbuoy's navigation system separately using the 'import attitude and position' functions of ESP3.

As the echosounder was mounted closer to the sea surface compared to traditional vessels, artifacts of bubble entrainment were observed in echograms as strong backscatter down to a maximum depth of ca. 5 m. We extracted these data and calculated the magnitude of these bubble entrainments (in a relative range of 0–1) as it expresses the extent of wave action and mixing of the surface layers (hereafter, near-surface turbulence), which may possess an ecological significance.

2.5.2. Noise reduction

Acoustic data were displayed as mean volume backscattering strength (S_v; dB re 1 m^{-1}) at a nominal frequency of 333 kHz. Due to increased attenuation at higher sound frequencies, we marked the acoustic data >100 m as a 'bad data' region. Since the influence of noise

<100 m was also notable, we used a built-in filtering algorithm in ESP3 for denoising. First, the filtering algorithm was applied across the entire data (S_v) region with a noise filtration threshold of −65 dB at 1 ping and 0.1 m resolution (see also Couperus et al., 2020). Although this resulted in a substantial reduction of noise, some intermittent noise remained, particularly at echogram depths below ca. 40 m. To reduce this, we built a Matlab® (Mathworks corp.) script that evaluates 0.1 m depth bins at each ping as,

$$(S_v)_{t,z} = \begin{cases} 'bad\ data' if \sum_{z=5}^{z} (s_v)_t > 0.70 \bullet \sum_{z=5}^{100} (s_v)_t \\ (S_v)_{t,z} if \sum_{z=5}^{z} (s_v)_t \le 0.70 \bullet \sum_{z=5}^{100} (s_v)_t \end{cases} \quad (2)$$

where,

$$(s_v)_{t,z} = 10^{\left[\frac{(S_v)_{t,z}}{10}\right]} \quad (3)$$

Here, t and z are time and depth and s_v (m^{-1}) is the linear volume backscattering strength. Data from the upper 5 m were discarded and vertical integrations of Eq. (2) were calculated from 5 m and downwards in order to exclude the area affected by bubble entrainment. Based on a number of trials, the cutoff value of 70% (Eq. (2)) proved to be the optimal in retaining 'good' data while filtering out the 'bad' data (see Appendix B for echograms before and after each denoising step).

2.5.3. Groundtruthing

To characterize acoustic categories and produce baseline estimates of their numerical abundance, we obtained data from the echosounder at the exact times when the two stations were sampled and when the Sailbuoy was closest to the sampling stations (Fig. 1). Once the acoustic data were pre-processed and denoised, we estimated the integrated s_v of the echogram regions corresponding to the times and depths of the MultiNet operations (i.e., one echogram region for each sampled depth layer). The integrated s_v was calculated across the employed frequency range (283–383 kHz) at 1 kHz resolution. Based on the relative composition of the taxa sampled with the MultiNet at each sampling date in each depth layer, we visually assigned three distinguishable S_v patterns in the echogram display to different taxonomic compositions. These 'acoustic categories' were further characterized using their frequency responses of S_v and target strength (*TS*, dB re 1 m^2, see results). The integrated s_v values were translated to numerical abundance (ind. m^{-3}) using the generic sound scattering models of Stanton et al. (1994). These calculations were solely based on the randomly oriented fluid-bent cylinder model (Stanton et al., 1993) because copepods, euphausiids and jellyfish accounted for most of the net-based numerical abundance (see results). Employing the Stanton et al. (1994) model, we used the mean body length and width measured for copepods, euphausiids and jellyfish captured in each net haul to estimate the mean backscattering cross-section (σ_{bs}) and mean *TS* and ultimately translated the s_v to numerical abundance in each sampled depth layer. Although the numerical abundances were estimated for each 1 kHz frequency band, the geometric mean over all frequencies was used in data presentation.

2.5.4. Scrutinizing and post-processing

During data processing, acoustic data along the Sailbuoy track were visualized at full display resolution (100% of the pings loaded) with low and high display thresholds (S_v) set between −75 dB and −25 dB. Echogram regions were then scrutinized for the three different acoustic categories identified in groundtruthing. To homogenize the accuracy of scrutinization, data of four hours were loaded at a time onto the echogram display, which was projected on a 49-in. ultrawide monitor with 32:9 (5120 × 1440 pixels) aspect ratio. Scrutinized echogram regions (s_v) were saved in grids of 1 s temporal and 1 m vertical resolution for each 1 kHz frequency band and were exported as Microsoft™ Excel® files using the 'export regions' command in ESP3.

Further processing of exported echogram regions was done in R™ version 3.6.2 using RStudio™ Integrated Development Environment (IDE) version 1.2.5033. Here, scrutinized data were binned into 1 h temporal and 1 m vertical resolution. This produced mean point estimates of s_v of different acoustic categories across the water column at the onset of each hour. The binned s_v of these acoustic categories were translated to numerical abundance (ind. m^{-3}) using their respective mean σ_{bs} and *TS* estimated during groundtruthing. Although the numerical abundances were estimated for each 1 kHz frequency band, the mean over all frequencies was used in the analyses below.

2.6. Vertical behavior and its environmental correlates

We interpreted the temporal changes of the hourly snapshots of vertically distributed abundance as vertical behavior. Due to the asynchrony of observed vertical behavior (see results), we did not correlate the hourly variability of the population centers (i.e., the weighted mean depth of the population at each hour: see Sørnes et al., 2007) with environmental variables. Instead, first, we estimated the percentage of the population (A) occupying each depth layer (z = 1 m) at each timepoint (t = 1 h) as,

$$A'_{t,z} = \frac{A_{t,z}}{\sum_{z=5}^{100} A_t}\% \quad (4)$$

Here, A_t is the total abundance at time t and $A_{t,z}$ is the estimated abundance at depth layer z at time t (ind. m^{-3}) where 5 and 100 are the minimum (i.e., to exclude the region of bubble entrainment) and maximum depths (m) used in this study. We then segregated the cumulative estimate of A'(%) at each 1-h timepoint into percentiles with 1% resolution from the near surface towards the maximum depth. Finally, we calculated the depths corresponding to each of these 1% percentiles.

We used Pearson's product moment correlation to describe linear associations between the hourly percentile depths of zooplankton and environmental variables, such as PAR, near-surface turbulence and the vertical distribution of potential predatory acoustic categories.

3. Results

3.1. Identities of sound scatterers – groundtruthing

The mean numerical abundance estimated using zooplankton net data and acoustic data (based on sound scattering models and body size estimates from net catches) aligned well, with the latter reaching up to ca. 60%–90% of the former (Fig. 2A, F). The shallow net haul (20–0 m) collected on 26 April had the highest zooplankton (and micronekton) numerical abundance, estimated at ca. 36000 ind. m^{-3} (Fig. 2A). *Calanus* spp. accounted for >82% of this abundance (Fig. 2B) with the vast majority (ca. 80%) being younger developmental stages consisting of nauplii and copepodites CI–CIII (Fig. 2C). In the echogram, this community was represented as relatively weak sound scatterers with S_v in the range of −65 and −75 dB (Fig. 2D). The mean abundance of the deeper net haul (50–20 m) collected on 26 April was ca. half of that of the shallower net haul and the community was again dominated by younger developmental stages of *Calanus* spp. (Fig. 2A–C). The drop in numerical abundance was evident in the echogram (S_v, Fig. 2D), but the backscattering strength did not change notably despite the proportional increase of smaller copepods (e.g., *Oithona* sp.) and early developmental stages of krill (*Thysanoessa* spp.) compared to the shallower net haul (Fig. 2B).

On 28 May, the mean abundance of the shallower net haul was estimated at ca. 28000 ind. m^{-3}, which almost exclusively (ca. 98%) composed of older developmental stages (CIV, CV and adults) of *Calanus*

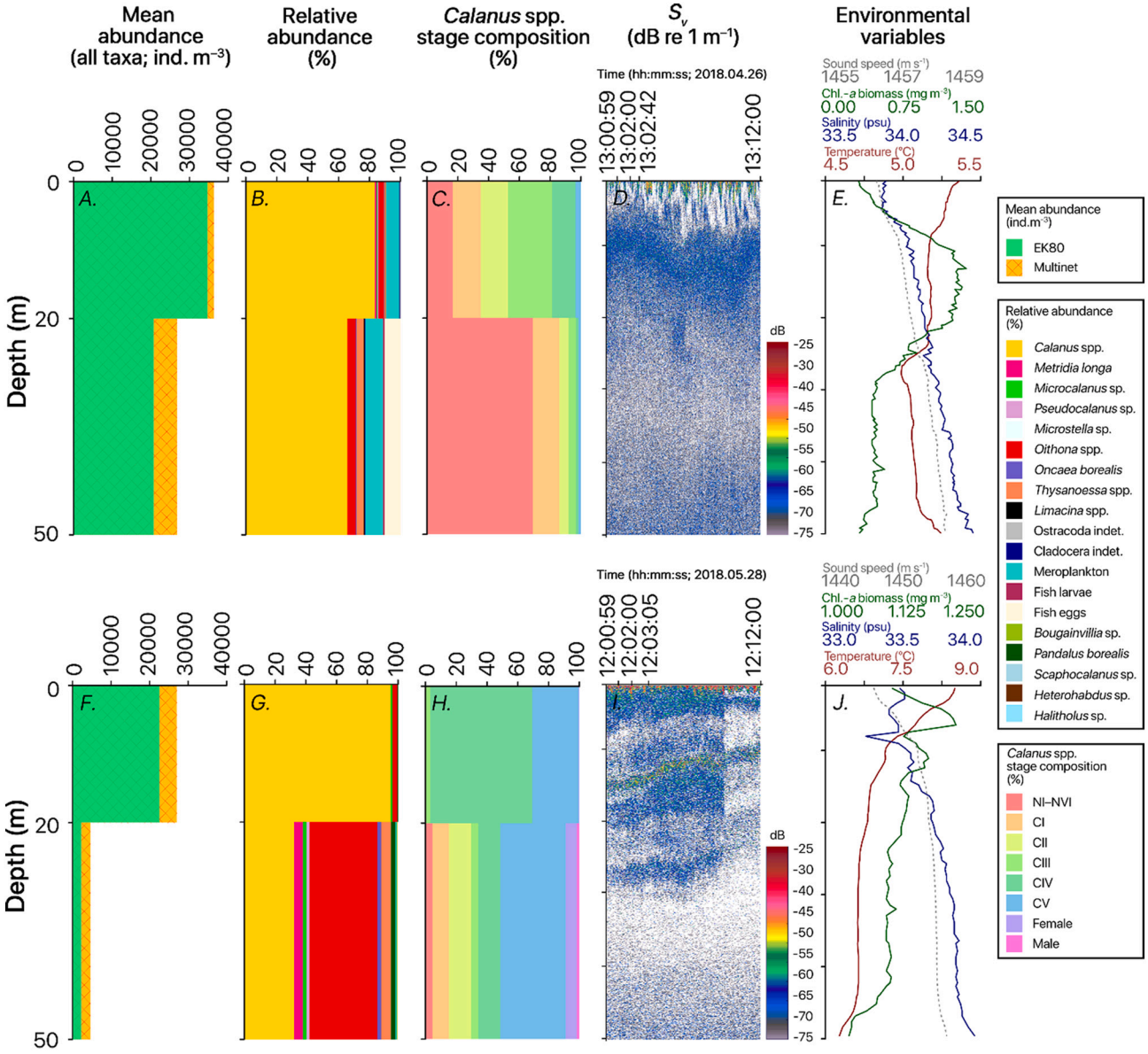

Fig. 2. Comparison of mean zooplankton and micronekton abundances and their vertical distributions estimated/observed from net samples and acoustic data collected at the two sampling stations, S1 (26 April 2018: panels A–D) and S2 (28 May 2018: panels F—I). Environmental variables profiled at these stations, which were used in the processing of acoustic data are plotted in panels E and J. See Fig. 1 for the location of the two sampling stations and corresponding positions of the Sailbuoy. Echograms (S_v, panels D & I) are for the nominal frequency of 333 kHz.

spp. with large lipid reserves (Fig. 2F, H). These larger individuals were clearly distinguishable in the echogram as a band of sound scatterers between 10 and 17 m depth that produced moderate S_v from −60 to −50 dB (Fig. 2I). There was a significant drop of numerical abundance in the deeper net haul on 28 May (estimated at <3000 ind. m^{-3}: Fig. 2F), which was clearly evident in the echogram (S_v, Fig. 2I). The increased community proportions of smaller copepods (e.g., *Oithona* spp., *Pseudocalanus* sp., *Microcalanus* sp., *Oncaea borealis*) produced the same weaker backscattering strength in this layer (in the range of −65 and −75 dB) as produced by younger developmental stages of *Calanus* spp. (cf. Fig. 2I & 2D).

The above groundtruthing led to the establishment of two main acoustic categories. The first included relatively weak sound scatterers (AC1: Fig. 3A) characterized by smaller copepods, younger developmental stages (CI–CIII) of larger copepods, i.e., *Calanus* spp. and larval stages of krill (estimated mean body length = 1.03 ± 0.88 mm and mean body width = 0.36 ± 0.39 mm). The second acoustic category included relatively moderate sound scatters (AC2: Fig. 3B) characterized by lipid-rich pre-adult and adult stages of *Calanus* spp. (estimated mean body length = 1.36 ± 0.81 mm and mean body width = 0.39 ± 0.20 mm). Apart from these two groups, we found a third acoustic category while browsing the data. These included relatively strong sound scatters producing S_v in a range of −45 to −35 dB (AC3: Fig. 3C). The taxonomic identity of AC3 could not be resolved as they were absent in the groundtruthing data. Attempts to quantify numerical abundance of AC3 using the body size estimates of AC2 resulted in producing extremely high and potentially unrealistic estimates, which often ranged up to 5×10^6 ind. m^{-3}. Due to the lack of groundtruthing data and owing to the sporadic presence of AC3 during the study period, we did not quantify their numerical abundance, but relied on their presence or absence in the analyses below. All acoustic categories identified in this study had prominent and distinguishable frequency responses of both *TS* and S_v (Fig. 3D–I).

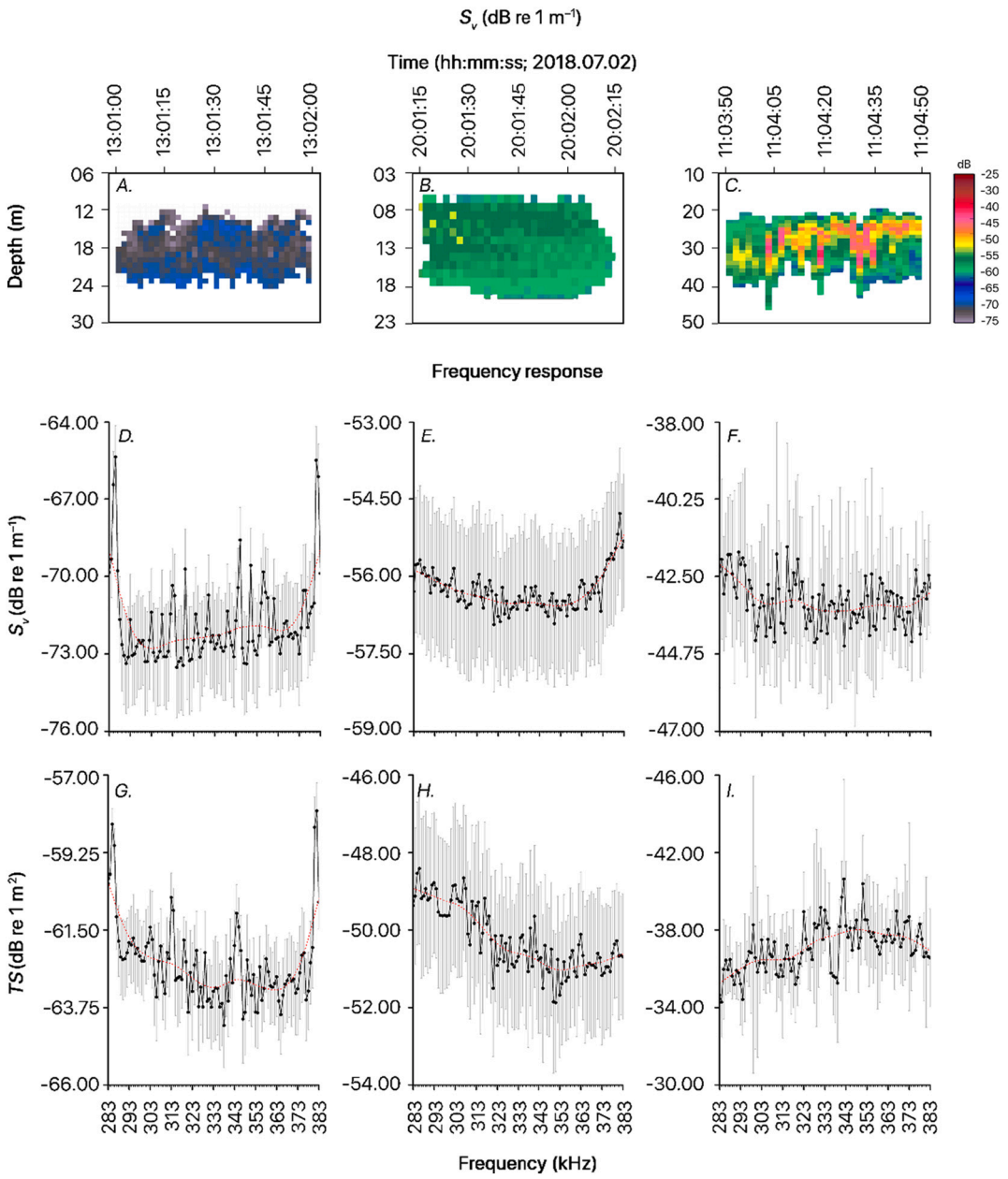

Fig. 3. Different echograms (S_v) and the frequency responses of S_v and *TS* of the three acoustic categories distinguished in this study (AC1: panels A, D, G; AC2: panels B, E, H and AC3: panels C, F, I). Dispersion bars of the frequency response panels (D—I) represent the standard deviation. Dotted red lines in those panels are locally weighted scatterplot smoothers (LOWESS) fitted to the data. (For interpretation of the references to color in this figure legend, the reader is referred to the web version of this article.)

3.2. Environmental dynamics

The near-surface temperature increased as the Sailbuoy travelled southwest from ca. 7.5 °C at the start of the study (29 June) to ca. 9.5 °C at the end of the study (10 July) (Fig. 4A). Between 29 June and 4 July, the near-surface salinity gradually increased from ca. 33.7 PSU to 34.7 PSU and remained largely constant thereafter (Fig. 4A). The sky was mostly cloudy during the entire voyage (Fig. 4B). The data indicated cloud-free skies and elevated surface irradiance for few hours from midday to midnight on 2 July, midnight to midday of 3 July and midday to midnight on 6 July (Fig. 4B, C). Irrespective of the time of the year and cloud attenuation, notable diel variation of irradiance was evident throughout the study period (Fig. 4C). Apart from a ca. two-day time window between 3 and 5 July, significant turbulence was detected in near-surface waters (Fig. 4D). The near-surface turbulence was most pronounced between 29 June–1 July and 7–9 July.

3.3. Abundance and vertical distribution of the zooplankton community

The maximum estimated numerical abundance (> 5 m depth) in the acoustic data was ca. 165,000 ind. m^{-3}. These high-density zooplankton aggregates corresponded to AC2 (older developmental stages of *Calanus* spp.), which occupied a depth range of 15–35 m during most of the study (Fig. 4E, F). In contrast, the estimated numerical abundance of AC1 remained <100,000 ind. m^{-3}. AC3 occurred intermittently, particularly during the first half of the survey (Fig. 4F).

The observed zooplankton community (AC1 and AC2) occupied the upper 50 m of the water column for most part of the survey. However, a notable deepening of their vertical distribution was noted at midday on the 29 and 30 June (Fig. 4F). Here, > 75% of the zooplankton

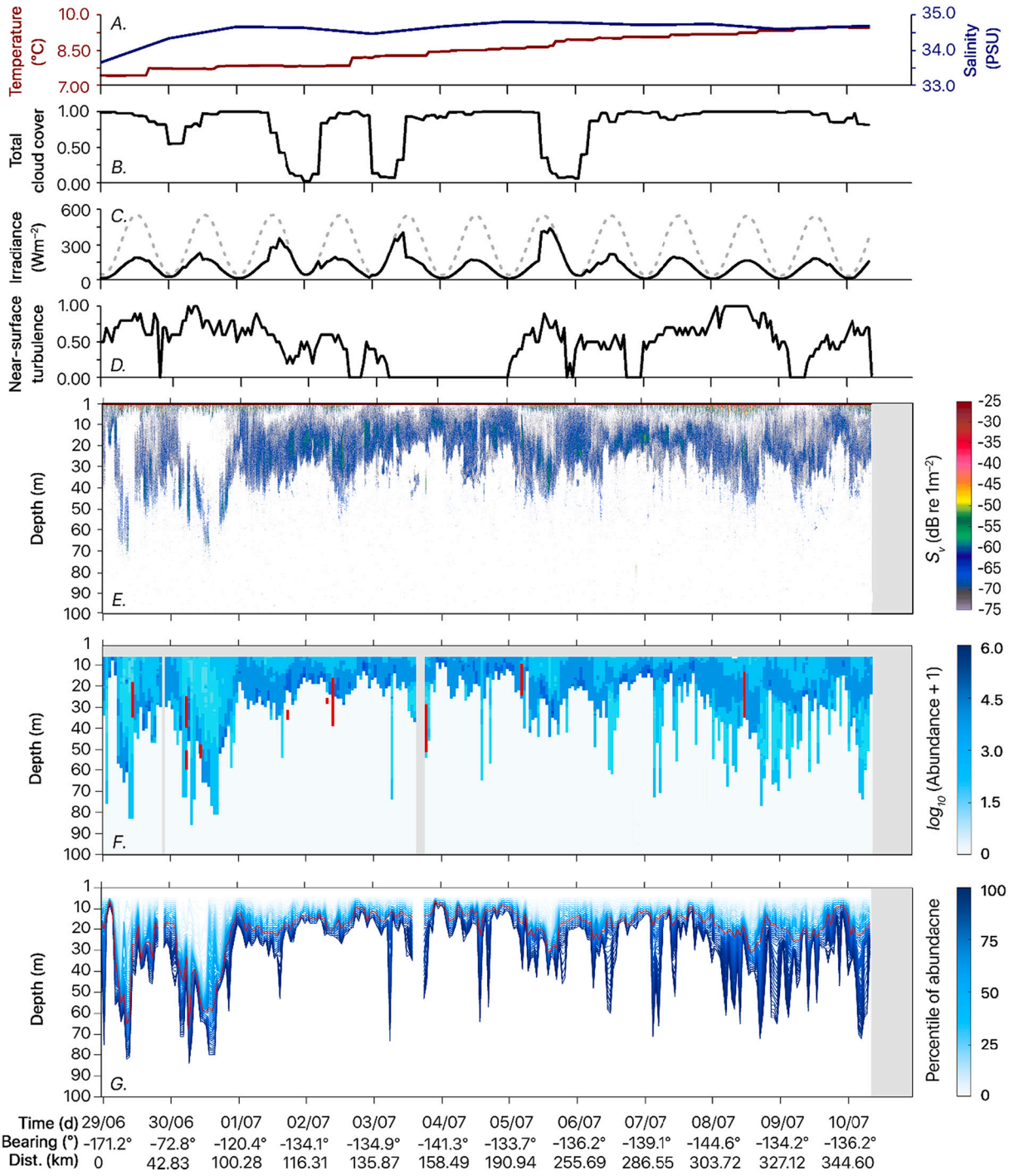

Fig. 4. Environmental dynamics (panels A–D), vertical distribution of denoised volume scattering strength (S_v, panel E: initial depth = transducer depth) and vertical distribution of estimated zooplankton abundance (logarithmic transformation, panel F) and its percentile depths (panel G) during the study period. Temperature and salinity (panel A) are denoted by red and blue lines, respectively. Dashed and solid lines (panel C) represent clear-sky and cloud-attenuated PAR, respectively. AC2 (older developmental stages of *Calanus* spp.) are indicated by the darkest blue color in panel F. The presence of AC3 (indeterminate taxon) is superimposed in red color. The rest of the abundance in panel F belongs to AC1 (smaller copepods and larval stages of krill). The red line in panel G represents the vertical distribution of 50th percentile of abundance. Cloud cover and near surface turbulence are on a relative scale (0–1). The approximate travel distance and bearing of the Sailbuoy at the onset of each date is given at the bottom. (For interpretation of the references to color in this figure legend, the reader is referred to the web version of this article.)

community was found below 50 m (Fig. 4G). A relatively less pronounced midday deepening of the vertical distribution was also noted on 1, 2, 5, 6 and 8–10 July, when >50% of the zooplankton community remained below 25–35 m (Fig. 4E–G). This midday deepening pattern co-oscillated with the daily light regime as indicated by the moderate to weak correlation ($0.35 > r > 0.20$) between zooplankton percentile depths (particularly up to the 30th percentile) and estimated surface irradiance (Fig. 5). Nine out of ten occurrences of AC3 (except on 3 July) either preceded or coincided with the midday deepening of the zooplankton community (AC1 and AC2) (Fig. 4F). The correlation between the occurrences of AC3 and the percentile depths of rest of the zooplankton was particularly notable between 15th and 35th percentiles

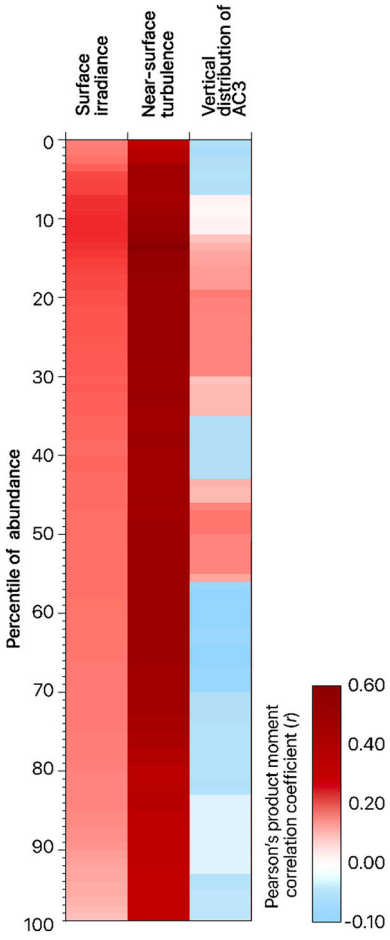

Fig. 5. Representation of linear association between each abundance percentile (1% resolution) and surface irradiance, near-surface turbulence and the vertical distribution of the unidentified acoustic category AC3 during the study period. Data presented as Pearson's product moment correlation coefficient (r). Metadata for the correlation tests are available in the Appendix C.

and 45th to 55th percentiles ($0.20 > r > 0.10$: Fig. 5). During the ca. 2-day window when the sky was cloudy and the near-surface waters was turbulence-free, most of the zooplankton community – smaller and larger taxa alike - was found above 20 m irrespective of the time of the day (Fig. 4E, F). However, whenever there was turbulence at the surface, the fraction of the community closer to the sea surface always retreated to depths >10 m irrespective of the time of the day, thus leaving empty white spaces on the echogram (Fig. 4E, cf. G). The influence of near-surface turbulence on the zooplankton community was evident throughout the water column, as shown by the moderate to strong correlations ($r > 0.25$) observed down to the 100th percentile of abundance (Fig. 5).

4. Discussion

By employing a silent surface vehicle with high-frequency acoustics we were able to observe the zooplankton community along the Norwegian Sea over a ca. 12-day mid-summer period. Groundtruthing based on depth-stratified zooplankton vertical net hauls enabled resolving the acoustic data into three different acoustic categories, which represented different taxonomic groups (Fig. 3). During most of the survey, the investigated zooplankton community occupied the upper 50 m (Fig. 4E). However, we observed periodic changes in their vertical distribution, which point to differential patterns of vertical behavior. A part of this vertical behavior on 29 & 30 June and 1, 2, 5, 6, 8–10 July (Fig. 4C, E–G) resembled the classic diel vertical migration of zooplankton (DVM), where zooplankton occupy near-surface waters during the night and retreat to deeper waters during the day (reviewed in Bayly, 1986; Brierley, 2014; Bandara et al., 2021). The observed classic DVM pattern on 29 and 30 June was particularly notable as most of the zooplankton community descended to depths below 50 m during daytime and ascended back during nighttime. In addition, we also observed a peculiar pattern of vertical behavior, which was driven by near-surface turbulence. Here, the zooplankton community retreated from near-surface waters in response to physical disturbances occurring at the sea surface, such as wave action and turbulent mixing (Fig. 4D–G). On cloudy days and in the absence of near-surface turbulence, we did not observe periodic vertical behavioral changes and most of the zooplankton community was concentrated in the upper 20 m of the water column (Fig. 4E–G).

4.1. Behavioral response to irradiance, cloud cover and food

The observed classic DVM pattern co-oscillated with the ambient irradiance as indicated by the respective weaker or moderately positive correlations in Fig. 5. Despite being mid-summer (period of midnight sun), notable diel variations of irradiance occurred throughout the study, irrespective of the attenuation by cloud cover (Fig. 4B, C). However, it is it appears that the observed classic DVM is not merely a light avoidance. This is because between 3 July and 5 July, when the daily surface light regime was quite similar to days on which DVM was observed, most of the zooplankton community was found in near-surface layers (Fig. 4B, C, E, F). This somewhat contrasts the recent findings of Hobbs et al. (2021) and Omand et al. (2021) that vertical distributions of zooplankton communities tend to follow subsurface irradiance intensities, where most individuals remain below preferred irradiance isolumes. However, unlike the above studies, we did not calculate the subsurface light levels and our behavior-environment correlates are solely based on surface irradiance estimates (Fig. 5). This is because precise estimates of subsurface irradiance require measurements, such as chlorophyll-*a* concentration, which was not profiled in this study. Further, the cloud cover and cloud-attenuated irradiance data (3-h estimates) may not have exactly matched the time window that the echosounder was operating (6 min at the onset of each hour) because of the ephemeral nature of cloud cover. While these limitations could have contributed to the discrepancy between our findings and those suggesting irradiance-driven vertical behavior, it appears that in addition to irradiance, there were other cues determining zooplankton vertical position (see below).

Periodically ascending to and occupation of near-surface layers is of particular relevance to predominantly herbivorous taxa, such as Subarctic and Arctic *Calanus* spp., which constituted the majority of the sampled zooplankton community (Fig. 2). These high-latitude copepods need to use the short productive season to maximize food intake to accumulate lipids in surface waters (Falk-Petersen et al., 2009). The phytoplankton bloom development in our study area typically commences in early April in near-surface waters (pre-bloom: mean upper 20 m Chl.-$a < 1$ mg m^{-3}) and advances to a full spring bloom (mean upper 20 m Chl.-$a > 2$ mg m^{-3}) by late May (Rey, 2004). Although bloom conditions gradually decrease towards summer, mean Chl.-*a* biomass >1 mg m^{-3} exist in the upper 10–20 m until a less conspicuous second algal bloom usually starts between late July and mid-August (Broms and Melle, 2007; Bagøien et al., 2012). Ocean color remote sensing (Copernicus-GlobColour: https://doi.org/10.48670/moi-00100) also indicate surface Chl.-*a* biomass between 0.5 and 6 mg m^{-3} along the Sailbuoy track during the study period (Appendix D). Therefore, there may have been a reasonable food supply for the herbivorous zooplankton in the near-surface waters during the study period. Food availability coupled with warmer ambient temperatures (Fig. 4A) creates a near-surface habitat with higher growth potential for these herbivorous planktonic ectotherms (Bandara et al., 2018). When the sea

surface remained calm between the midday of 3 July and midnight of 5 July, > 50% of the zooplankton community was found in the upper 20 m of the water column (Fig. 4D–G). Despite the surface irradiance levels during this period being similar to those of 29 and 30 June, unlike those days, no significant DVM was observed. Instead, even relatively large individuals (AC2, i.e., older developmental stages of *Calanus* spp.) were found in the upper 20 m irrespective of the time of the day (Fig. 4E, F). Since the sky was fully cloud-covered during this period (Fig. 4B), it is likely that zooplankton (predominantly herbivores) used this calm time window to occupy relatively warm, food-rich near-surface waters to elevate feeding opportunities free of physical disturbance.

4.2. Behavioral response to predators

A plausible explanation of the observed DVM is that zooplankton of the study area used diel variations of irradiance as a proximate cue for performing DVM to minimize visual predator encounters. This is in line with previous findings from freshwater and nearshore marine environments (reviewed in Bandara et al., 2021). Unless threatened by visual predators, zooplankton tend to occupy these near-surface layers to elevate their growth and development rates (Bollens and Frost, 1989a; Hays et al., 2001). Several, but not all, of the pronounced midday descents of zooplankton (i.e., on 29–30 June and 8–9 July, Fig. 4E-G) occurred in the presence of the strongly sound scattering acoustic category (AC3). The study area is one of the prime summertime feeding grounds of Northeast Arctic cod (*Gadus morhua*), Norwegian spring-spawning herring (*Clupea harengus*) and Northeast Atlantic Mackerel (*Scomber scombrus*), which collectively exert a substantial predation risk on larger copepods and euphausiids (Sundby, 2000; Dommasnes et al., 2004; Bachiller et al., 2016). Net samples collected at the two stations had many eggs and few larval Atlantic cod (*G. morhua*) (Fig. 2), whose diet mainly comprise of copepods (Conover et al., 1995). However, the lack of trawl data and other operational frequencies of the echosounder do not allow for a confident characterization of AC3. The strong response of the zooplankton community to the presence of AC3 in combination with the known planktivorous predators in the area strongly suggests that AC3 were planktivorous fish (in particular, their larval stages).

4.3. Behavioral response to near-surface turbulence

During the Beagle survey voyage, Charles Darwin noted that planktonic organisms tend to disappear from near-surface layers during periods of strong wave action (Darwin, 1833). Currently, there is a wealth of empirical evidence indicating that zooplankton of both marine and freshwater origin tend to retreat to calmer deeper layers (sometimes abandoning their routine DVM behavior) when the near-surface turbulence is pronounced (e.g., Garcia-Soto et al., 1990; Visser et al., 2001; Maar et al., 2006; Baranyai et al., 2011). It is suggested that this avoidance behavior mainly reflects the negative impact of higher turbulence on the feeding efficiency of zooplankton (Kiørboe and Saiz, 1995; Visser and Stips, 2002). Similar to these findings, our acoustic observations indicate that zooplankton vertical distributions along the Sailbuoy's route were strongly associated with the near-surface turbulence (Figs. 4D–G & 5). Predictions from Météo-France Wave Model (MFWAM, based on historical altimetry missions and directional wave spectra from Synthetic Aperture Radar from Sentinel 1 satellite: https://doi.org/10.48670/moi-00022) indicate that the high near-surface turbulences detected by the echosounder between 28 and 30 June and 7–10 July were due to waves with an average height of ca. 2.0–2.7 m breaking on the sea surface (Appendix E). Although the turbulence was restricted to the upper 5 m of the water column (indicated by bubble entrainments in the echogram: Fig. 4D, E), its impact was evident across most of the zooplankton community occupying all depth layers (Fig. 5). That is, when the shallower layers of zooplankton reacted to near-surface turbulence by retreating to depths (down to 10 m: Fig. 4E), it somehow triggered a similar behavior among zooplankton occupying relatively deeper waters (Figs. 4E–G & 5). Although this somewhat resembles the schooling behavior of fish (reviewed in Pavlov and Kasumyan, 2000), it is not clear how such a behavior with high-level synchronization would persist in a multispecies aggregate of zooplankton. The calculated correlation coefficients accounted for 25%–55% of the linear associations between the percentile depths and near-surface turbulence (Fig. 5, Appendix C). Therefore, it could be that not the whole zooplankton community – but only one or few of the dominant taxa, such as *Oithona* spp. and *Calanus* spp. were responsible for this schooling-like behavior. Both these taxa are known to vertically migrate (descend) when near-surface turbulence is pronounced (Visser et al., 2001; Maar et al., 2006). Further, *Calanus* spp. have been observed in near-surface dense swarms (Ambler, 2002; Basedow et al., 2019) and recent experiments indicate a concerted response of *Calanus* individuals to downwelling fluxes, thus hinting at some behavioral synchrony within these swarms (Weidberg et al., 2021). Synchronized swimming and schooling behaviors are well-known for krill species of both southern (Antarctic) and northern (North Atlantic and Arctic) origins (e.g., Hamner and Hamner, 2000; McQuinn et al., 2015). Further, smaller copepods, such as *Labidocera pavo* can exert high-level schooling behavior (i.e., synchronized swimming, distancing and orientating patterns) under physical disturbance (Omori and Hamner, 1982). Therefore, the observed downward migration in response to surface turbulence could be a response by a group of *Oithona* or *Calanus* spp. – but their ability to perform schooling behavior warrants further investigations.

4.4. Advantages and limitations of technologies used in this study

The Sailbuoy implemented in this study has a smaller profile and thus allowed the echosounder transducer to be mounted at a shallow depth (ca. at 0.5 m below the waterline). This allows the echosounder to cover a broader range extending from closer to the surface towards its maximum operational range. In contrast, echosounders affixed to conventional research vessels are usually mounted several meters below the waterline and hence do not profile the near-surface layers. Further, the Sailbuoy was free of engine noise due to its wind-driven operation. Consequently, we could interpret bubble entrainment artifacts in the acoustic data solely as near-surface turbulence. The silent and dark operation of the Sailbuoy may also have aided in artifact-free characterization of near-surface zooplankton layers since they can react to noise, vibrations and artificial lights of research vessels and retreat to depths (Berge et al., 2020; Geoffroy et al., 2021). However, the presence of near-surface turbulence masked the zooplankton abundance in the upper 5 m in the acoustic data (Fig. 4E). Although this led to the removal of the upper 5 m of zooplankton data in the analyses, our findings show that the impact of near-surface turbulence had behaviorally resonated all the way down to 50–70 m across the zooplankton community (Fig. 5). Acoustic artifacts of bubble entrainment can thus be used in the vertical behavior studies of zooplankton.

One key strength of echosounder data is the higher spatio-temporal resolution and coverage it encompass (reviewed in Wiebe and Benfield, 2003; Bandara et al., 2021). Nonetheless, the temporal coverage of our data was somewhat hampered by the limited (ca. 10%) duty cycle of the echosounder implemented as a storage- and power-saving feature. Our hourly vertical distribution snapshots were thus based on ca. 6 min of returning echoes at the onset of each hour. Although this seems suboptimal, such snapshot-type vertical distribution characterizations are not uncommon in plankton ecology. For example, many DVM interpretations are still based on diurnal snapshots of zooplankton vertical distributions, where a duplet of net hauls is collected at midday and midnight (see Pearre, 1979 for a critical review). A standard zooplankton net (e.g., MultiNet or WP-2 net) towed at 0.5 m s^{-1} (Fraser, 1968) would have traversed the usable operational range of the echosounder used in our study (ca. 100 m) in <1 min. Assuming diurnal

replicates, a classic net-based study would extrapolate this <1 min zooplankton vertical distribution data over a period of 12 h (as 'daytime' or 'nighttime' distributions) thus accounting for a duty-cycle equivalent of <0.14%. In comparison, our acoustic data had nearly an order of magnitude more temporal coverage. Future developments in hardware will likely further increase the duty cycle and hence the temporal coverage of the data.

Comparison of numerical abundances estimated from net samples and acoustic data (Fig. 2) shows that the operational frequencies used in this study (283–383 kHz) are suitable for the detection of mesozooplankton, such as the Subarctic and Arctic *Calanus* spp. and perhaps micronekton, such as early developmental stages of larval cod (Fig. 3 & see also Chu et al., 2003; Pedersen et al., 2019). Although exact species distinctions from acoustic signals are still not possible, our groundtruthing shows that these higher-frequency broadband signals are useful in characterizing the *Calanus* community and differentiation of developmental stages. However, numerical abundances estimated from acoustic data were solely based on a single sound scattering model (fluid-bent cylinder model: Stanton et al., 1993). Our net samples did not capture sufficient marine gastropods to obtain an accurate estimation of their body size and to implement the spherical elastic shell model (Stanton et al., 1994). Further, despite a diversity of meroplankton taxa, such as worm-like forms (e.g., polychaetes) and shelled forms (e.g., bivalves) were captured in the net samples (Fig. 2), sound scattering models are not widely available for acoustic estimation of their abundance. These limitations may have led to an underestimation of numerical abundance in the observed zooplankton community (cf. abundance estimate comparisons in Fig. 2). In addition, the higher sound frequencies employed in this study may be sub-optimal for detecting adult krill and chaetognaths, which produce stronger backscatter at <125 kHz and ca. 200 kHz respectively (Holliday and Pieper, 1980; Darnis et al., 2017). Lower sound frequencies (< 200 kHz) are also desirable in detection of planktivorous fish, such as Atlantic herring and mackerel (e.g., Korneliussen and Ona, 2003; Gorska et al., 2004).

4.5. Conclusion

The silent surface vehicle used in this study allowed us to characterize how the observed vertical behavior of zooplankton varied throughout the study period in response to several environmental variables, and in particular, how copepods responded to near surface disturbances and potential predators. The inability of the autonomous surface vehicle to profile the water column did not allow us to reconstruct the subsurface irradiance, temperature, salinity and food availability dynamics (for herbivorous zooplankton), which may have added further to the present interpretations. Future deployments should thus aim towards the synchronized (coupled) use of surface and underwater vehicles (e.g., Van et al., 2020). In addition to the profiling of subsurface environmental dynamics, such coupled operations allow seamless (near-real-time) groundtruthing of the acoustic data if a photographic or videographic plankton identification system is mounted on the underwater vehicle (e.g., Ohman et al., 2019). Seamlessly groundtruthed acoustic data will be more accurate in predicting the identities of the sound scatters, their abundance and vertical distribution than described in this study, in which the groundtruthing area is outside of the Sailbuoy track. Despite the limitations of the present approach, our findings shed new light on summertime vertical behavior of high-latitude zooplankton. We therefore envision substantial merit in the use of in-situ plankton observation systems (acoustics and optics) on board autonomous platforms.

Declaration of Competing Interest

The authors declare that they have no known competing financial interests or personal relationships that could potentially influence the research reported in this paper.

Acknowledgments

This work was funded by the project GLIDER – unmanned ocean vehicles, a flexible and cost-efficient offshore monitoring and data-management approach (project no. 269188/E30) and project "Collaborative Studies of Two Resource Ecosystems in Shelf, Slope an Oceanic Regions of the Norwegian and South China Seas (Stressor)", funded by the Norwegian Research Council (project no. 287043). Geir Pedersen's contribution was partially funded by CRIMAC (Norwegian Research Council project no. 309512). We thank Morten Krogstad for the technical help rendered during the collection of zooplankton net samples. Further, we express our gratitude to the two reviewers and the co-editor-in-chief Prof. Eileen Hofmann for reading the earlier draft of this manuscript and suggesting improvements.

Appendix A. Supplementary data

Supplementary data to this article can be found online at https://doi.org/10.1016/j.jmarsys.2022.103733.

References

Ambler, J.W., 2002. Zooplankton swarms: characteristics, proximal cues and proposed advantages. Hydrobiologia 480, 155–164.
Bachiller, E., Skaret, G., Nøttestad, L., Slotte, A., 2016. Feeding ecology of Northeast Atlantic Mackerel, Norwegian Spring-Spawning Herring and Blue Whiting in the Norwegian Sea. PLoS One 11, e0149238.
Bagøien, E., Melle, W., Kaartvedt, S., 2012. Seasonal development of mixed layer depths, nutrients, chlorophyll and *Calanus finmarchicus* in the Norwegian Sea – A basin-scale habitat comparison. Prog. Oceanogr. 103, 58–79.
Bandara, K., Varpe, Ø., Ji, R., Eiane, K., 2018. A high-resolution modeling study on diel and seasonal vertical migrations of high-latitude copepods. Ecol. Model. 368, 357–376.
Bandara, K., Varpe, Ø., Wijewardene, L., Tverberg, V., Eiane, K., 2021. Two hundred years of zooplankton vertical migration research. Biol. Rev. 96, 1547–1589.
Baranyai, E., Vári, A., Homonnay, Z., 2011. The effect of variable turbulent intensities on the distribution of zooplankton in the shallow, large Lake Balaton (Hungary). Knowl. Manag. Aquat. Ecosyst. 400, 07.
Basedow, S.L., Edvardsen, A., Tande, K.S., 2008. Vertical segregation of *Calanus finmarchicus* copepodites during the spring bloom. J. Mar. Syst. 70, 21–32.
Basedow, S.L., Tande, K.S., Stige, L.C., 2010. Habitat selection by a marine copepod during the productive season in the Subarctic. Mar. Ecol. Prog. Ser. 416, 165–178.
Basedow, S.L., McKee, D., Lefering, I., Gislason, A., Daase, M., Trudnowska, E., Egeland, E.S., Choquet, M., Falk-Petersen, S., 2019. Remote sensing of zooplankton swarms. Sci. Rep. 9, 1–10.
Båtnes, A.S., Miljeteig, C., Berge, J., Greenacre, M., Johnsen, G.H., 2015. Quantifying the light sensitivity of *Calanus* spp. during the polar night: potential for orchestrated migrations conducted by ambient light from the sun, moon, or aurora borealis? Polar Biol. 38, 51–65.
Baumgartner, M.F., Tarrant, A.M., 2017. The physiology and ecology of diapause in marine copepods. Annu. Rev. Mar. Sci. 9, 387–411.
Bayly, I.A.E., 1986. Aspects of diel vertical migration in zooplankton, and its enigma variations. In: De Deckker, P., Williams, W.D. (Eds.), Limnology in Australia. Springer, Netherlands, Dordrecht, pp. 349–368.
Berge, J., Geoffroy, M., Daase, M., Cottier, F., Priou, P., Cohen, J.H., Johnsen, G., McKee, D., Kostakis, I., Renaud, P.E., 2020. Artificial light during the polar night disrupts Arctic fish and zooplankton behaviour down to 200 m depth. Commun. Biol. 3, 1–8.
Berrisford, P., Dee, D., Poli, P., Brugge, R., Fielding, K., Fuentes, M., Kallberg, P., Kobayashi, S., Uppala, S., Simmons, A., 2011. The ERA-Interim archive, Version 2.0. European Centre for Medium Range Weather Forecasts, Berkshire, United Kingdom.
Blachowiak-Samolyk, K., Kwasniewski, S., Richardson, K., Dmoch, K., Hansen, E., Hop, H., Falk-Petersen, S., Mouritsen, L.T., 2006. Arctic zooplankton do not perform diel vertical migration (DVM) during periods of midnight sun. Mar. Ecol. Prog. Ser. 308, 101–116.
Bollens, S.M., Frost, B.W., 1989a. Predator-induced diel vertical migration in a planktonic copepod. J. Plankton Res. 11, 1047–1065.
Bollens, S.M., Frost, B.W., 1989b. Zooplanktivorous fish and variable diel vertical migration in the marine planktonic copepod *Calanus pacificus*. Limnol. Oceanogr. 34, 1072–1083.
Brierley, A.S., 2014. Diel vertical migration. Curr. Biol. 24, R1074–R1076.
Broms, C., Melle, W., 2007. Seasonal development of *Calanus finmarchicus* in relation to phytoplankton bloom dynamics in the Norwegian Sea. Deep-Sea Res. II Top. Stud. Oceanogr. 54, 2760–2775.
Campbell, J.W., Aarup, T., 1989. Photosynthetically available radiation at high latitudes. Limnol. Oceanogr. 34, 1490–1499.
Chu, D., Wiebe, P.H., Copley, N.J., Lawson, G.L., Puvanendran, V., 2003. Material properties of North Atlantic cod eggs and early-stage larvae and their influence on acoustic scattering. ICES J. Mar. Sci. 60, 508–515.

Cohen, J.H., Forward, R.B., 2002. Spectral sensitivity of vertically migrating marine copepods. Biol. Bull. 203, 307–314.
Cohen, J.H., Forward, R., 2009. Zooplankton diel vertical migration—a review of proximate control. Oceanogr. Mar. Biol. Annu. Rev. 47 (47), 77–110.
Conover, R.J., Wilson, S., Harding, G.C., Vass, W.P., 1995. Climate, copepods and cod: some thoughts on the long-range prospects for a sustainable northern cod fishery. Clim. Res. 5, 69–82.
Cottier, F.R., Tarling, G.A., Wold, A., Falk-Petersen, S., 2006. Unsynchronised and synchronised vertical migration of zooplankton in a high Arctic fjord. Limnol. Oceanogr. 51, 2586–2599.
Couperus, B., Sakinan, S., Burggraaf, D., 2020. Small Pelagic Fish and Zooplankton in the Dutch Coastal Surf Zone during the EGS-II Survey in 2017-2018. Wageningen Marine Research, Wageningen, The Netherlands.
Darnis, G., Hobbs, L., Geoffroy, M., Grenvald, J.C., Renaud, P.E., Berge, J., Cottier, F., Kristiansen, S., Daase, M., E. Søreide, J., Wold, A., Morata, N., Gabrielsen, T., 2017. From polar night to midnight sun: diel vertical migration, metabolism and biogeochemical role of zooplankton in a high Arctic fjord (Kongsfjorden, Svalbard). Limnol. Oceanogr. 62, 1586–1605.
Darwin, C., 1833. Charles Darwin's Diary of the Voyage of H.M.S. "Beagle". Macmillan Publishers, New York, USA.
Dini, M.L., Carpenter, S.R., 1992. Fish predators, food availability and diel vertical migration in *Daphnia*. J. Plankton Res. 14, 359–377.
Dommasnes, A., Melle, W., Dalpadado, P., Ellertsen, B., 2004. Herring as a major consumer in the Norwegian Sea. ICES J. Mar. Sci. 61, 739–751.
Falk-Petersen, S., Mayzaud, P., Kattner, G., Sargent, J.R., 2009. Lipids and life strategy of Arctic *Calanus*. Mar. Biol. Res. 5, 18–39.
Folt, C.L., Burns, C.W., 1999. Biological drivers of zooplankton patchiness. Trends Ecol. Evol. 14, 300–305.
Francois, R., Garrison, G., 1982. Sound absorption based on ocean measurements. Part II: Boric acid contribution and equation for total absorption. J. Acoust. Soc. Am. 72, 1879–1890.
Fraser, J., 1968. Standardization of zooplankton sampling methods at sea. In: Tranter, J. (Ed.), Zooplankton Sampling, Part II. UNESCO Press, Paris, pp. 149–168. The United Nations Educational, Scientific and Cultural Organization, Paris, France.
Garcia-Soto, C., de Madariaga, I., Villate, F., Orive, E., 1990. Day-to-day variability in the plankton community of a coastal shallow embayment in response to changes in river runoff and water turbulence. Estuar. Coast. Shelf Sci. 31, 217–229.
Geoffroy, M., Langbehn, T., Priou, P., Varpe, Ø., Johnsen, G., Le Bris, A., Fisher, J.A., Daase, M., McKee, D., Cohen, J., 2021. Pelagic organisms avoid white, blue, and red artificial light from scientific instruments. Sci. Rep. 11, 1–13.
Gjøsæter, H., 1995. Pelagic fish and the ecological impact of the modern fishing industry in the Barents Sea. Arctic 48, 267–278.
Gorska, N., Ona, E., Korneliussen, R.J., 2004. On Acoustic Multi-Frequency Species Identification and Separation of Atlantic Mackerel, Norwegian Spring Spawn Herring and Norway Pout, M 2004/R:18. ICES, Copenhagen, Denmark, pp. 1–9.
Hamner, W.M., Hamner, P.P., 2000. Behavior of Antarctic krill (*Euphausia superba*): schooling, foraging, and antipredatory behavior. Can. J. Fish. Aquat. Sci. 57, 192–202.
Hays, G.C., Kennedy, H., Frost, B.W., 2001. Individual variability in diel vertical migration of a marine copepod: why some individuals remain at depth when others migrate? Limnol. Oceanogr. 46, 2050–2054.
Hobbs, L., Banas, N.S., Cohen, J.H., Cottier, F.R., Berge, J., Varpe, Ø., 2021. A marine zooplankton community vertically structured by light across diel to interannual timescales. Biol. Lett. 17, 20200810.
Holliday, D., Pieper, R., 1980. Volume scattering strengths and zooplankton distributions at acoustic frequencies between 0.5 and 3 MHz. J. Acoust. Soc. Am. 67, 135–146.
Kiørboe, T., Saiz, E., 1995. Planktivorous feeding in calm and turbulent environments, with emphasis on copepods. Mar. Ecol. Prog. Ser. 122, 135–145.
Korneliussen, R.J., Ona, E., 2003. Synthetic echograms generated from the relative frequency response. ICES J. Mar. Sci. 60, 636–640.
Ladroit, Y., Escobar-Flores, P.C., Schimel, A.C., O'Driscoll, R.L., 2020. ESP3: An open-source software for the quantitative processing of hydro-acoustic data. SoftwareX 12, 100581.
Lampert, W., 1989. The adaptive significance of diel vertical migration of zooplankton. Funct. Ecol. 3, 21–27.
Loose, C.J., Dawidowicz, P., 1994. Trade-offs in diel vertical migration by zooplankton: the costs of predator avoidance. Ecology 75, 2255–2263.
Maar, M., Visser, A., Nielsen, T.G., Stips, A., Saito, H., 2006. Turbulence and feeding behaviour affect the vertical distributions of *Oithona similis* and *Microsetella norwegica*. Mar. Ecol. Prog. Ser. 313, 157–172.
McQuinn, I.H., Plourde, S., St. Pierre, J.-F., Dion, M., 2015. Spatial and temporal variations in the abundance, distribution, and aggregation of krill (*Thysanoessa raschii* and *Meganyctiphanes norvegica*) in the lower estuary and Gulf of St. Lawrence. Prog. Oceanogr. 131, 159–176.
Moseidjord, H., Svenden, H., Slagstad, D., Båmstedt, U., 1999. Sensitivity studies of circulation and ocean-shelf exchange off northen Norway. Sarsia 84, 191–198.
Ohman, M., 1988. Behavioral responses of zooplankton to predation. Bull. Mar. Sci. 43, 530–550.
Ohman, M., Davis, R.E., Sherman, J.T., Grindley, K.R., Whitmore, B.M., Nickels, C.F., Ellen, J.S., 2019. Zooglider: an autonomous vehicle for optical and acoustic sensing of zooplankton. Limnol. Oceanogr. Methods 17, 69–86.
Omand, M.M., Steinberg, D.K., Stamieszkin, K., 2021. Cloud shadows drive vertical migrations of deep-dwelling marine life. Proc. Natl. Acad. Sci. 118, e2022977118.
Omori, M., Hamner, W., 1982. Patchy distribution of zooplankton: behavior, population assessment and sampling problems. Mar. Biol. 72, 193–200.
Pavlov, D., Kasumyan, A., 2000. Patterns and mechanisms of schooling behavior in fish: a review. J. Ichthyol. 40, S163.
Pearre, S., 1979. Problems of detection and interpretation of vertical migration. J. Plankton Res. 1, 29–44.
Pedersen, G., Falk-Petersen, S., Dunlop, K., Camus, L., Daase, M., Basedow, S.L., Bandara, K., Tverberg, V., Pederick, J., Peddie, D., 2019. Autonomous surface vehicles for persistent acoustic monitoring of zooplankton in a highly productive shelf area. In: OCEANS 2019-Marseille. IEEE, pp. 1–7.
Price, H., Paffenhöfer, G.-A., Boyd, C., Cowles, T., Donaghay, P., Hamner, W., Lampert, W., Quetin, L., Ross, R., Strickler, J., 1988. Future studies of zooplankton behavior: questions and technological developments. Bull. Mar. Sci. 43, 853–872.
Rey, F., 2004. Phytoplankton: the grass of the sea. In: Skjoldal, H.R., Sætre, R. (Eds.), The Norwegian Sea Ecosystem. Tapir Academic Press, Trondheim, Norway, pp. 97–136.
Robledo, L., Soler, A., 2000. Luminous efficacy of global solar radiation for clear skies. Energy Convers. Manag. 41, 1769–1779.
Saiz, E., 2009. Swimming dynamics of zooplankton. In: Duarte, C., Helgueras, A. (Eds.), Encyclopedia of Life. Eolss Publishers, Oxford, UK, pp. 319–338.
Sakshaug, E., Johnsen, G.H., Kristiansen, S., von Quillfeldt, C., Rey, F., Slagstad, D., Thingstad, F., 2009. Phytoplankton and Primary Production. In: Sakshaug, E., Johnsen, G.H., Kovacs, K.M. (Eds.), Ecosystem Barents Sea. Tapir Academic Press, Trondheim, Norway, pp. 167–209.
Seuront, L.G., Brewer, M.C., Strickler, J.R., 2004. Quantifying zooplankton swimming behavior: the question of scale. In: Seuront, L.G., Strutton, P.G. (Eds.), Handbook of Scaling Methods in Aquatic Ecology: Measurement, Analysis, Simulation. CRC Press, Florida, USA, pp. 333–359.
Skarðhamar, J., Svendsen, H., 2005. Circulation and shelf–ocean interaction off North Norway. Cont. Shelf Res. 25, 1541–1560.
Sørnes, T.A., Aksnes, D.L., Båmstedt, U., Youngbluth, M.J., 2007. Causes for mass occurrences of the jellyfish *Periphylla periphylla*: a hypothesis that involves optically conditioned retention. J. Plankton Res. 29, 157–167.
Stanton, T.K., Chu, D., Wiebe, P.H., Clay, C.S., 1993. Average echoes from randomly oriented random-length finite cylinders: zooplankton models. J. Acoust. Soc. Am. 94, 3463–3472.
Stanton, T.K., Wiebe, P.H., Chu, D., Benfield, M.C., Scanlon, L., Martin, L., Eastwood, R. L., 1994. On acoustic estimates of zooplankton biomass. ICES J. Mar. Sci. 51, 505–512.
Stich, H.B., Lampert, W., 1984. Growth and reproduction of migrating and non-migrating *Daphnia* species under simulated food and temperature conditions of diurnal vertical migration. Oecologia 61, 192–196.
Sundby, S., 1984. Influence of bottom topography on the circulation at the continental shelf off northern Norway. Fiskeridirektoratets Skrifter Serie Havundersøkelser 17, 501–519.
Sundby, S., 2000. Recruitment of Atlantic cod stocks in relation to temperature and advectlon of copepod populations. Sarsia 85, 277–298.
Vadstein, O., 2009. Interactions in the planktonic food web. In: Sakshaug, E., Johnsen, G. H., Kovacs, K.M. (Eds.), Ecosystem Barents Sea. Tapir Academic Press, Trondheim, Norway, pp. 251–266.
Van, M., Bui, D.H.P., Do, Q.T., Huynh, T.-T., Lee, S.-D., Choi, H.-S., 2020. Study on dynamic behavior of unmanned surface vehicle-linked unmanned underwater vehicle system for underwater exploration. Sensors 20, 1329.
Visser, A.W., Stips, A., 2002. Turbulence and zooplankton production: insights from PROVESS. J. Sea Res. 47, 317–329.
Visser, A., Saito, H., Saiz, E., Kiørboe, T., 2001. Observations of copepod feeding and vertical distribution under natural turbulent conditions in the North Sea. Mar. Biol. 138, 1011–1019.
Wallace, M.I., Cottier, F.R., Berge, J., Tarling, G.A., Griffiths, C., Brierley, A.S., 2010. Comparison of zooplankton vertical migration in an ice-free and a seasonally ice-covered Arctic fjord: an insight into the influence of sea ice cover on zooplankton behavior. Limnol. Oceanogr. 55, 831–845.
Weidberg, N., DiBacco, C., Pezzola, C., Rebiffe, E., Basedow, S.L., 2021. Swimming performance of subarctic *Calanus* spp. facing downward currents. Mar. Ecol. Prog. Ser. 665, 47–61.
Wiebe, P.H., Benfield, M.C., 2003. From the Hensen net toward four-dimensional biological oceanography. Prog. Oceanogr. 56, 7–136.
Williamson, C.E., Fischer, J.M., Bollens, S.M., Overholt, E.P., Breckenridge, J.K., 2011. Toward a more comprehensive theory of zooplankton diel vertical migration: integrating ultraviolet radiation and water transparency into the biotic paradigm. Limnol. Oceanogr. 56, 1603–1623.
Wilson, W.D., 1960. Speed of sound in sea water as a function of temperature, pressure, and salinity. J. Acoust. Soc. Am. 32, 641–644.